INT. J. CONTROL, 2003, VOL. 76, NO. 14, 1420–1427

Velocity control of robot manipulators: analysis and experiments

JAVIER MORENO† and RAFAEL KELLY†*

This paper addresses the velocity control of robot manipulators in joint space, assuming Lagrangian non-linear dynamics, by three control schemes resulting as extensions of proportional-integral velocity regulators of direct current motors. The feasibility of these control strategies is evaluated through experiments on a two degree-of-freedom direct-drive arm.

1. Introduction

Velocity regulation and velocity control of electrical motors have many applications in industrial processes and machine tools. The objective of velocity *regulation* is to maintain the velocity of the motor shaft to a given constant desired reference. In contrast, the goal of velocity *control* is to track accurately a time-varying desired velocity.

Velocity control of electromechanical systems is an active research topic in linear and non-linear control. Robust velocity control of a permanent magnet direct current (DC) motor has been addressed in Bonivento *et al*. (1994) using an outer velocity loop based on a modified binary feedback of integral type and an inner current controller operating in sliding mode. Kim *et al*. (1997) reported experimental comparisons between two non-linear controllers for speed regulation of current-fed induction motors which preserve the proportional-integral (PI) velocity loop structure. Recently, a learning control method for the high-precision velocity control of servo motors in the presence of disturbance torque was proposed in Han *et al*. (1998). This control scheme consists of a PI controller plus a feedforward term for disturbance rejection.

Velocity control is also an important theoretical and practical issue in robotic manipulators. The concept of kinematic control (Canudas de Wit *et al*. 1996) deals with the end-effector pose (position and orientation) control based on the assumption that the robot joint velocities are the manipulator's inputs. This assumption may hold only when suitable velocity controllers are incorporated to drive each robot joint. The actual situation in many industrial robots is that the control of each axis is carried out making use of an inner velocity loop in addition to an outer position loop (Corke 1994, Nilsson 1996). These velocity loops arise from individual velocity regulators of the corresponding electrical motors where feedforward compensation is added to handle disturbances due to manipulator non-linear dynamics (Luh 1983). On the other hand, joint velocity control is also a key issue in force control of robot manipulators where better performance can be achieved using velocity commands instead of position or direct torque commands (De Schutter *et al*. 1997).

The objective of this paper is to analyse and evaluate three approaches for joint velocity control of manipulators. These controllers belong to the model-based class because they depend on the corresponding robot non-linear dynamics but have the nice feature that they result as natural extensions of the PI velocity error feedback plus acceleration feedforward commonly utilized for velocity control of DC motors. These control schemes were originally designed to solve the motion control problem, i.e. for tracking time-varying desired joint positions. They correspond to the inverse dynamics controller (Spong and Vidyasagar 1989), also called computed-torque technique, the PD control with compensation controller (Slotine and Li 1991) and the PD+ controller (Koditschek 1984). The adaptation of these controllers to solve the joint velocity control problem is made straightforward by introducing the integral of the velocity error in lieu of the standard joint position error—which is nonsense in velocity control formulation because no specification of the desired joint position is involved.

As a second contribution of this paper, we present the experimental evaluation of the velocity controllers on a two degree-of-freedom direct-drive arm. Direct-drive robots—those robots without transmission mechanisms from the motor shafts to links—offer the interesting challenge of their non-linear dynamics. Advantages of such a class of robots are the absence of backslash and high stiffness, all of which are helpful for applications in fast and accurate motions (Asada *et al*. 1983).

This paper is organized as follows. Section 2 is devoted to summarizing the DC motor model and robot dynamics. The control strategies for joint velocity control of robotic manipulators are analysed in § 3. Experimental results are presented in § 4. Finally, in § 5 we offer brief concluding remarks.

Received 15 February 2002. Revised 12 May 2003.
* Author for correspondence. e-mail: rkelly@cicese.mx
† División de Física Aplicada, CICESE, Apdo. Postal 2615, Adm. 1, Ensenada, B.C., 22800, Mexico.

International Journal of Control ISSN 0020–7179 print/ISSN 1366–5820 online
http://www.tandf.co.uk/journals
DOI: 10.1080/00207170310001593010

2. DC motor and robot dynamics

A classical linear description of an armature-controlled DC motor—neglecting armature inductance—is given by (Ogata 1970, Kuo 1982, Spong and Vidyasagar 1989)

$$J\ddot{q} + \left[f + \frac{K_a K_b}{R_a}\right]\dot{q} = \frac{K_a}{R_a} v \tag{1}$$

where q is the shaft angular position, v is the voltage input, J is the rotor inertia and f is the viscous friction. The constants K_a, K_b and R_a are electrical characteristics of the motor.

Velocity *regulation* in DC motors is often achieved by PI velocity error feedback. Let $\dot{q}_d$ be the desired angular velocity which is for the moment assumed constant. The velocity *regulation* aim is to ensure that the velocity shaft $\dot{q}$ reaches asymptotically the desired velocity, i.e. $\lim_{t\to\infty} \dot{q}(t) = \dot{q}_d$. This control objective can be attained by a simple PI velocity control law given by

$$v = k_v \dot{\tilde{q}} + k_i z \tag{2}$$

$$\dot{z} = \dot{\tilde{q}} \tag{3}$$

where $\dot{\tilde{q}}$ stands for the velocity error defined by $\dot{\tilde{q}} = \dot{q}_d - \dot{q}$, and k_v and k_i are positive constants called proportional and integral gains.

The velocity *control* formulation, where the objective is to track a time-varying desired velocity $\dot{q}_d$, can be easily resolved by the PI velocity regulator (2) and (3) by taking care of damping compensation and adding a feedforward term of the desired acceleration $\ddot{q}_d$, that is

$$v = k_v \dot{\tilde{q}} + k_i z + \frac{R_a}{K_a}\left[f + \frac{K_a K_b}{R_a}\right]\dot{q} + J\frac{R_a}{K_a}\ddot{q}_d \tag{4}$$

$$\dot{z} = \dot{\tilde{q}} \tag{5}$$

It is worth remarking that the following control law where the desired velocity $\dot{q}_d$ is used in lieu of the actual velocity $\dot{q}$ for 'damping compensation'

$$v = k_v \dot{\tilde{q}} + k_i z + \frac{R_a}{K_a}\left[f + \frac{K_a K_b}{R_a}\right]\dot{q}_d + J\frac{R_a}{K_a}\ddot{q}_d \tag{6}$$

also achieves asymptotic velocity tracking.

On the other hand, the dynamics of a serial n-link robot manipulator can be written as (Spong and Vidyasagar 1989)

$$M(\boldsymbol{q})\ddot{\boldsymbol{q}} + C(\boldsymbol{q}, \dot{\boldsymbol{q}})\dot{\boldsymbol{q}} + \boldsymbol{g}(\boldsymbol{q}) = \boldsymbol{\tau} \tag{7}$$

where $\boldsymbol{q}$ is the $n \times 1$ vector of joint displacements, $\dot{\boldsymbol{q}}$ is the $n \times 1$ vector of joint velocities, $\boldsymbol{\tau}$ is the $n \times 1$ vector of applied torque inputs, $M(\boldsymbol{q})$ is the $n \times n$ symmetric positive definite manipulator inertia matrix, $C(\boldsymbol{q}, \dot{\boldsymbol{q}})\dot{\boldsymbol{q}}$ is the $n \times 1$ vector of centripetal and Coriolis torques,† and $\boldsymbol{g}(\boldsymbol{q})$ is the $n \times 1$ vector of gravitational torques due to the gravity.

The matrix $C(\boldsymbol{q}, \dot{\boldsymbol{q}})$—defined by using the Christoffel symbols—and the time derivative of the inertia matrix $\dot{M}(\boldsymbol{q})$ satisfy (Koditschek 1984, Spong and Vidyasagar 1989)

$$\boldsymbol{x}^{\mathrm{T}}\left[\tfrac{1}{2}\dot{M}(\boldsymbol{q}) - C(\boldsymbol{q}, \dot{\boldsymbol{q}})\right]\boldsymbol{x} = 0 \qquad \forall \boldsymbol{x}, \boldsymbol{q}, \dot{\boldsymbol{q}} \in \mathbb{R}^n \tag{8}$$

and

$$\dot{M}(\boldsymbol{q}) = C(\boldsymbol{q}, \dot{\boldsymbol{q}}) + C^{\mathrm{T}}(\boldsymbol{q}, \dot{\boldsymbol{q}}) \qquad \forall \boldsymbol{q}, \dot{\boldsymbol{q}} \in \mathbb{R}^n \tag{9}$$

Similar to velocity control of DC motors, the formulation of velocity control of robots in joint coordinates starts from a desired joint velocity vector $\dot{\boldsymbol{q}}_d(t)$ which is assumed to be bounded and continuously differentiable. The velocity control objective is to drive the robot arm in such a way that the velocity error $\dot{\tilde{\boldsymbol{q}}} = \dot{\boldsymbol{q}}_d - \dot{\boldsymbol{q}}$ vanishes asymptotically, i.e.

$$\lim_{t\to\infty} \dot{\tilde{\boldsymbol{q}}}(t) = \lim_{t\to\infty} [\dot{\boldsymbol{q}}_d(t) - \dot{\boldsymbol{q}}(t)] = \boldsymbol{0}$$

The structure of the robot dynamics (7) can be seen as a generalization of the DC motor model (1). Specifically, the robot model captures the DC model structure when

$$M(\boldsymbol{q}) = \frac{R_a}{K_a} J \tag{10}$$

$$C(\boldsymbol{q}, \dot{\boldsymbol{q}}) = \frac{R_a}{K_a}\left[f + \frac{K_a K_b}{R_a}\right] \tag{11}$$

$$\boldsymbol{g}(\boldsymbol{q}) = \boldsymbol{0} \tag{12}$$

The main objective of the paper is to study velocity controllers for robotic manipulators having the characteristic of reduction to the DC motor velocity control structure (4) and (5) under conditions (10)–(12).

3. Velocity control

Three velocity controllers for robot manipulators are presented in this section. They correspond to adaptation of well-known motion controllers (joint position tracking controllers) where an integral action of the velocity error is introduced in the controllers to eliminate the nonsense position error signal. This modification yields an underlying PI velocity error feedback loop.

† Viscous friction defined as a linear function of velocity can be added to $C(\boldsymbol{q}, \dot{\boldsymbol{q}})$.

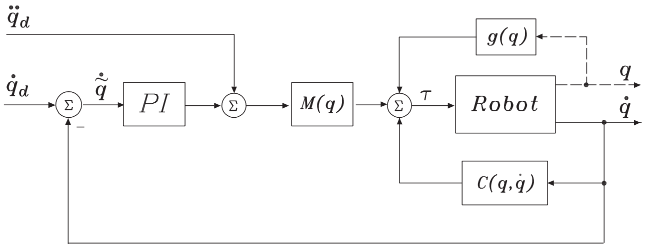

Figure 1. Velocity control based on inverse dynamics.

3.1. *Inverse dynamics control*

The inverse dynamics control of robot manipulators—but replacing the integral of the velocity error $\dot{\tilde{\boldsymbol{q}}}$ instead of the 'position error'—is given by

$$\boldsymbol{\tau} = M(\boldsymbol{q})\left[\ddot{\boldsymbol{q}}_d + K_v\dot{\tilde{\boldsymbol{q}}} + K_i\boldsymbol{z}\right] + C(\boldsymbol{q},\dot{\boldsymbol{q}})\dot{\boldsymbol{q}} + \boldsymbol{g}(\boldsymbol{q}) \qquad (13)$$

$$\dot{\boldsymbol{z}} = \dot{\tilde{\boldsymbol{q}}} \qquad (14)$$

where K_v and K_i denote $n \times n$ symmetric positive definite matrices. A block diagram is depicted in figure 1.

Considering conditions (10) and (11), the control law (13) and (14) becomes (4) and (5) where

$$k_v I = \frac{R_a}{K_a} J K_v$$

$$k_i I = \frac{R_a}{K_a} J K_i$$

Substituting the controller (13) and (14) into the robot dynamics (7), we obtain the closed-loop system

$$\frac{\mathrm{d}}{\mathrm{d}t}\begin{bmatrix} \boldsymbol{z} \\ \dot{\tilde{\boldsymbol{q}}} \end{bmatrix} = \begin{bmatrix} \dot{\tilde{\boldsymbol{q}}} \\ -K_v\dot{\tilde{\boldsymbol{q}}} - K_i\boldsymbol{z} \end{bmatrix}$$

which is globally asymptotically stable because K_i and K_v are symmetric positive definite matrices. To prove this, we borrow the Lyapunov function (Wen and Bayard 1988)

$$V(\boldsymbol{z},\dot{\tilde{\boldsymbol{q}}}) = \tfrac{1}{2}\left[\dot{\tilde{\boldsymbol{q}}} + \varepsilon\boldsymbol{z}\right]^{\mathrm{T}}\left[\dot{\tilde{\boldsymbol{q}}} + \varepsilon\boldsymbol{z}\right] + \tfrac{1}{2}\boldsymbol{z}^{\mathrm{T}}\left[K_i + \varepsilon K_v - \varepsilon^2 I\right]\boldsymbol{z}$$

where ε is any constant satisfying† $0 < \varepsilon < \lambda_m\{K_v\}$. Under this condition we have that matrices $K_v - \varepsilon I$ and $K_i + \varepsilon K_v - \varepsilon^2 I$ are positive definite. The time derivative of $V(\boldsymbol{z},\dot{\tilde{\boldsymbol{q}}})$ along the trajectories of the closed-loop system yields

$$\dot{V}(\boldsymbol{z},\dot{\tilde{\boldsymbol{q}}}) = -\dot{\tilde{\boldsymbol{q}}}^{\mathrm{T}}[K_v - \varepsilon I]\dot{\tilde{\boldsymbol{q}}} - \varepsilon\, \boldsymbol{z}^{\mathrm{T}} K_i \boldsymbol{z}$$

which is a globally negative definite function. Therefore, the Lyapunov's direct method can be invoked to have the conclusion of global asymptotic stability, hence we have that the velocity error $\dot{\tilde{\boldsymbol{q}}}$ vanishes asymptotically, that is $\lim_{t\to\infty}\dot{\tilde{\boldsymbol{q}}}(t) = \boldsymbol{0}$ for any initial condition $\boldsymbol{z}(0)$ and $\dot{\tilde{\boldsymbol{q}}}(0)$.

† In this paper $\lambda_m\{A\}$ denote the minimum eigenvalue of a symmetric matrix A.

3.2. *PD control with compensation*

The PD control with compensation corresponds to the non-adaptive version of the controller introduced by Slotine and Li (1991). By utilizing the integral of the velocity error $\dot{\tilde{\boldsymbol{q}}}$ in lieu of the 'position error', the resulting control law can be rewritten as

$$\boldsymbol{\tau} = M(\boldsymbol{q})\left[\ddot{\boldsymbol{q}}_d + \Lambda\dot{\tilde{\boldsymbol{q}}}\right] + C(\boldsymbol{q},\dot{\boldsymbol{q}})[\dot{\boldsymbol{q}}_d + \Lambda\boldsymbol{z}] + \boldsymbol{g}(\boldsymbol{q}) + K_v\dot{\tilde{\boldsymbol{q}}} + K_i\boldsymbol{z} \qquad (15)$$

$$\dot{\boldsymbol{z}} = \dot{\tilde{\boldsymbol{q}}} \qquad (16)$$

where K_i and K_v denote $n \times n$ positive definite matrices and $\Lambda = K_v^{-1}K_i$. The block diagram corresponding to this controller is shown in figure 2.

This control strategy has the nice feature of reducing to the PI control structure (5) and (6) for the DC motor under conditions (10)–(12) with

$$k_v I = \frac{R_a}{K_a} J\Lambda + K_v$$

$$k_i I = \frac{R_a}{K_a}\left[f + \frac{K_a K_b}{R_a}\right]\Lambda + K_i$$

The closed-loop system obtained by substituting the control law (15) and (16) into the robot model (7) can be written as

$$\frac{\mathrm{d}}{\mathrm{d}t}\begin{bmatrix} \boldsymbol{z} \\ \dot{\tilde{\boldsymbol{q}}} \end{bmatrix} = \begin{bmatrix} \dot{\tilde{\boldsymbol{q}}} \\ M(\boldsymbol{q})^{-1}\left[-C(\boldsymbol{q},\dot{\boldsymbol{q}})\left[\dot{\tilde{\boldsymbol{q}}} + \Lambda\boldsymbol{z}\right] - K_v\dot{\tilde{\boldsymbol{q}}} - K_i\boldsymbol{z}\right] - \Lambda\dot{\tilde{\boldsymbol{q}}} \end{bmatrix} \qquad (17)$$

where

$$\boldsymbol{q}(t) = \int_0^t \dot{\boldsymbol{q}}_d(\sigma)\,\mathrm{d}\sigma - \boldsymbol{z}(t) + \boldsymbol{q}(0)$$

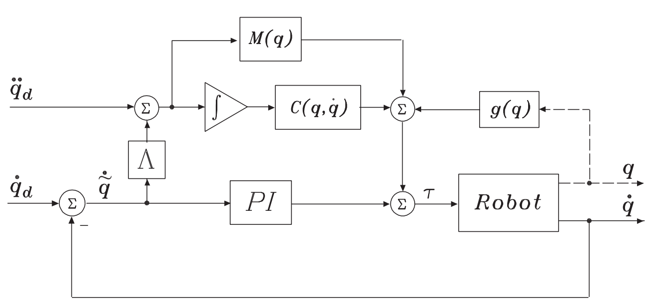

Figure 2. Velocity control based on PD control with compensation.

Equation (17) is non-linear and non-autonomous, but the origin of the state space is an equilibrium point. Global asymptotic stability of this equilibrium can be demonstrated by means of the following strict Lyapunov function inspired from Spong *et al.* (1990)

$$V(\boldsymbol{z},\dot{\tilde{\boldsymbol{q}}}) = \tfrac{1}{2}\left[\dot{\tilde{\boldsymbol{q}}} + \Lambda \boldsymbol{z}\right]^{\mathrm{T}} M(\boldsymbol{q})\left[\dot{\tilde{\boldsymbol{q}}} + \Lambda \boldsymbol{z}\right] + \boldsymbol{z}^{\mathrm{T}} K_i \boldsymbol{z}$$

After some simplifications and evoking (8), the time derivative $\dot{V}(\boldsymbol{z},\dot{\tilde{\boldsymbol{q}}})$ results

$$\dot{V}(\boldsymbol{z},\dot{\tilde{\boldsymbol{q}}}) = -\dot{\tilde{\boldsymbol{q}}}^{\mathrm{T}} K_v \dot{\tilde{\boldsymbol{q}}} - \boldsymbol{z}^{\mathrm{T}} K_i K_v^{-1} K_i \boldsymbol{z}$$

Because the matrix $K_i K_v^{-1} K_i$ is positive definite, hence the time derivative of the Lyapunov function is globally negative definite. Therefore, the Lyapunov's direct method guarantees that the closed-loop system is globally asymptotically stable. In turn, the velocity control objective is attained, that is, $\dot{\tilde{\boldsymbol{q}}}(t) \to 0$ as $t \to \infty$ for any initial condition.

3.3. *PD+ control*

The PD+ control scheme proposed by Koditschek (1984) to solve the motion control of robotic manipulators can be adjusted to address the joint velocity control by substituting the 'position error' signal by the integral of the velocity error $\dot{\tilde{\boldsymbol{q}}}$. This approach yields the control law

$$\boldsymbol{\tau} = M(\boldsymbol{q})\ddot{\boldsymbol{q}}_d + C(\boldsymbol{q},\dot{\boldsymbol{q}})\dot{\boldsymbol{q}}_d + \boldsymbol{g}(\boldsymbol{q}) + K_v \dot{\tilde{\boldsymbol{q}}} + K_i \boldsymbol{z} \quad (18)$$

$$\dot{\boldsymbol{z}} = \dot{\tilde{\boldsymbol{q}}} \quad (19)$$

where K_v are K_i are symmetric positive definite matrices. See figure 3 for a block diagram of this control strategy.

This control technique also preserves the PI control structure (5) and (6) for the DC motor under conditions (10)–(12) with $k_v I = K_v$ and $k_i I = K_i$.

The closed-loop system obtained by substituting the control law (18) and (19) into the model (7) is given by

$$\frac{\mathrm{d}}{\mathrm{d}t}\begin{bmatrix} \boldsymbol{z} \\ \dot{\tilde{\boldsymbol{q}}} \end{bmatrix} = \begin{bmatrix} \dot{\tilde{\boldsymbol{q}}} \\ M(\boldsymbol{q})^{-1}\left[-C(\boldsymbol{q},\dot{\boldsymbol{q}})\dot{\tilde{\boldsymbol{q}}} - K_v \dot{\tilde{\boldsymbol{q}}} - K_i \boldsymbol{z}\right] \end{bmatrix} \quad (20)$$

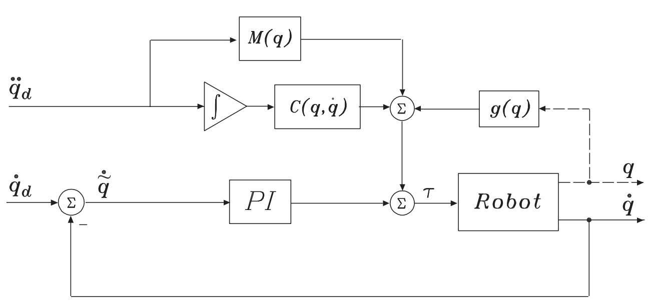

Figure 3. Velocity control based on PD+ control approach.

Although this differential equation is non-linear and non-autonomous, it can be verified that the origin of the state space is an equilibrium point.

The stability analysis can be carried out by invoking the Lyapunov's direct method using the following Lyapunov function candidate (Santibañez and Kelly 1997)

$$V(\boldsymbol{z},\dot{\tilde{\boldsymbol{q}}}) = \tfrac{1}{2}\dot{\tilde{\boldsymbol{q}}} M(\boldsymbol{q})\dot{\tilde{\boldsymbol{q}}} + \tfrac{1}{2}\boldsymbol{z}^{\mathrm{T}} K_i \boldsymbol{z} + \gamma \boldsymbol{f}(\boldsymbol{z})^{\mathrm{T}} M(\boldsymbol{q})\dot{\tilde{\boldsymbol{q}}}$$

where γ is a sufficiently small positive constant and $\boldsymbol{f}(\boldsymbol{z})$ is defined as

$$\boldsymbol{f}(\boldsymbol{z}) = \frac{1}{1 + \|\boldsymbol{z}\|}\boldsymbol{z}$$

In virtue of (8) and (9), the time derivative of $V(\boldsymbol{z},\dot{\tilde{\boldsymbol{q}}})$ along the trajectories of the closed-loop system (20) becomes

$$\begin{aligned}\dot{V}(\boldsymbol{z},\dot{\tilde{\boldsymbol{q}}}) = &-\dot{\tilde{\boldsymbol{q}}}^{\mathrm{T}} K_v \dot{\tilde{\boldsymbol{q}}} + \gamma \dot{\boldsymbol{f}}(\boldsymbol{z})^{\mathrm{T}} M(\boldsymbol{q})\dot{\tilde{\boldsymbol{q}}} \\ &- \gamma \boldsymbol{f}(\boldsymbol{z})^{\mathrm{T}} K_i \boldsymbol{z} - \gamma \boldsymbol{f}(\boldsymbol{z})^{\mathrm{T}} K_v \dot{\tilde{\boldsymbol{q}}} + \gamma \boldsymbol{f}(\boldsymbol{z})^{\mathrm{T}} C(\boldsymbol{q},\dot{\boldsymbol{q}})^{\mathrm{T}} \dot{\tilde{\boldsymbol{q}}}\end{aligned}$$

Following the arguments presented in Santibañez and Kelly (1997) it can be shown that $\dot{V}(\boldsymbol{z},\dot{\tilde{\boldsymbol{q}}})$ is globally negative definite provided that γ is small enough. Thus, global asymptotic stability is guaranteed.

4. Experimental results

We have designed and built a direct-drive arm with two vertical rigid links (see figure 4). High torque, brushless direct-drive motors operating in torque mode are used to drive the joints without gear reduction. A motion control board based on a TMS320C31 32-bit floating point microprocessor from Texas Instruments is used to execute the control algorithm. The control program is written in C programming language executed in the control board at $h = 2.5$ (ms) sampling period. The capability of the motor 1 is 200 (Nm) and the motor 2 is 15 (Nm).

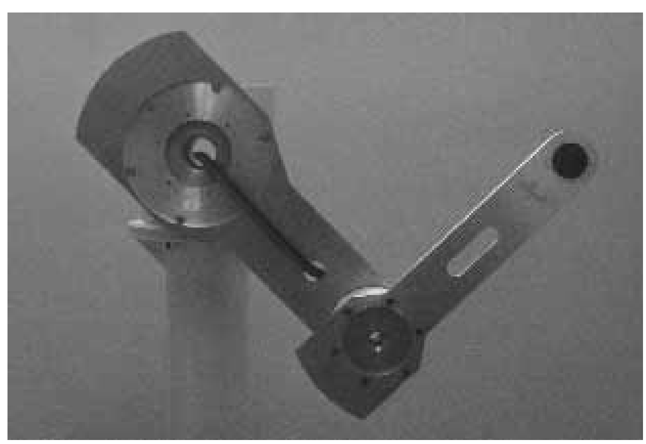

Figure 4. Experimental robot arm.

	Notation	Value	Unit
Length link 1	l_1	0.45	m
Length link 2	l_2	0.45	m
Link (1) centre of gravity	l_{c1}	0.091	m
Link (2) centre of gravity	l_{c2}	0.048	m
Mass link 1	m_1	23.90	kg
Mass link 2	m_2	3.88	kg
Inertia link 1	I_1	1.27	kg/m^2
Inertia link 2	I_2	0.09	kg/m^2
Gravity acceleration	g	9.8	m/s^2

Table 1. Parameters of the manipulator.

With reference to the symbols listed in table 1, we present below the entries of the robot dynamics (Reyes and Kelly 1997, 2001).

The elements $M_{ij}(\boldsymbol{q})$ $(i, j = 1, 2)$ of the inertia matrix $M(\boldsymbol{q})$ are

$$M_{11}(\boldsymbol{q}) = m_1 l_{c1}^2 + m_2\left[l_1^2 + l_{c2}^2 + 2l_1 l_{c2}\cos(q_2)\right] + I_1 + I_2$$

$$M_{12}(\boldsymbol{q}) = m_2\left[l_{c2}^2 + l_1 l_{c2}\cos(q_2)\right] + I_2$$

$$M_{21}(\boldsymbol{q}) = m_2\left[l_{c2}^2 + l_1 l_{c2}\cos(q_2)\right] + I_2$$

$$M_{22}(\boldsymbol{q}) = m_2 l_{c2}^2 + I_2$$

The elements $C_{ij}(\boldsymbol{q}, \dot{\boldsymbol{q}})$ $(i, j = 1, 2)$ from the centrifugal and Coriolis matrix $C(\boldsymbol{q}, \dot{\boldsymbol{q}})$ are

$$C_{11}(\boldsymbol{q}, \dot{\boldsymbol{q}}) = -m_2 l_1 l_{c2}\sin(q_2)\dot{q}_2$$

$$C_{12}(\boldsymbol{q}, \dot{\boldsymbol{q}}) = -m_2 l_1 l_{c2}\sin(q_2)[\dot{q}_1 + \dot{q}_2]$$

$$C_{21}(\boldsymbol{q}, \dot{\boldsymbol{q}}) = m_2 l_1 l_{c2}\sin(q_2)\dot{q}_1$$

$$C_{22}(\boldsymbol{q}, \dot{\boldsymbol{q}}) = 0$$

The entries of the gravitational torque vector $\boldsymbol{g}(\boldsymbol{q})$ are given by

$$g_1(\boldsymbol{q}) = [m_1 l_{c1} + m_2 l_1]g\sin(q_1) + m_2 l_{c2} g\sin(q_1 + q_2)$$

$$g_2(\boldsymbol{q}) = m_2 l_{c2} g\sin(q_1 + q_2)$$

Experiments showed that static and Coulomb friction at the motor joints are present and they depend in a complex manner on the joint position and velocity. We have decided to compensate only viscous friction and the remaining friction terms act as disturbance of the closed-loop system. The viscous friction terms have the form

$$f_1(\dot{\boldsymbol{q}}) = b_1\dot{q}_1$$

$$f_2(\dot{\boldsymbol{q}}) = b_2\dot{q}_2$$

where the coefficients have been estimated as $b_1 = 2.288$ [N ms] and $b_2 = 0.175$ [N ms], for the joints 1 and 2, respectively.

4.1. *Desired velocity trajectory and performance criterion*

The desired velocity trajectory $\dot{\boldsymbol{q}}_d(t)$ used in all experiments is given by

$$\dot{\boldsymbol{q}}_d(t) = \begin{bmatrix} 4.71t^2\,\mathrm{e}^{-2t^3} + 1.05t^2\,\mathrm{e}^{-2t^3}\sin(15t) + 2.62[1 - \mathrm{e}^{-2t^3}]\cos(15t) \\ 5.65t^2\,\mathrm{e}^{-1.8t^3} + 11.78t^2\,\mathrm{e}^{-1.8t^3}\sin(3.5t) + 7.64[1 - \mathrm{e}^{-1.8t^3}]\cos(3.5t) \end{bmatrix} \quad (\text{rad/s}) \qquad (21)$$

With regard to the desired velocity (21), it is easy to show that its components satisfy

$$|\dot{q}_{d1}(t)| \le 149.5, \quad (\text{deg/s}) \qquad (22)$$

$$|\dot{q}_{d2}(t)| \le 437.2, \quad (\text{deg/s}) \qquad (23)$$

for all $t \ge 0$.

The time evolution of the velocity error $\dot{\tilde{\boldsymbol{q}}}$ reflects how well the control system performance is. The performance criterion considered in this paper was the root mean square (RMS) value of the velocity error truncated Euclidean norm on a trip of time T, that is

$$\mathcal{L}_T^2[\dot{\tilde{\boldsymbol{q}}}] = \sqrt{\frac{1}{T}\int_0^T \|\dot{\tilde{\boldsymbol{q}}}(\sigma)\|^2\,\mathrm{d}\sigma} \quad (\text{rad/s}) \qquad (24)$$

The $\mathcal{L}_T^2$ norm has been previously evoked by several authors as a criterion of tracking performance (De Jager and Banens 1994, Jaritz and Spong 1996, Reyes and Kelly 2001). In practice, the discrete implementation of the criterion (24) leads to

$$\mathcal{L}_T^2[\dot{\tilde{\boldsymbol{q}}}] = \sqrt{\frac{1}{T}\sum_{k=0}^{T/h}\|\dot{\tilde{\boldsymbol{q}}}(kh)\|^2\, h} \quad (\text{rad/s})$$

where $h = 2.5$ (ms) is the sampling period and $T = 10$ (s) is the trip time.

4.2. *Inverse dynamics control*

The inverse dynamics control (13) and (14) was implemented with the gains

$$K_i = \mathrm{diag}\{1000, 5000\} \quad (1/\mathrm{s}^2)$$

$$K_v = \mathrm{diag}\{63.25, 141.42\} \quad (1/\mathrm{s})$$

Figure 5 depicts the components $\dot{\tilde{q}}_1$ and $\dot{\tilde{q}}_2$ of the joint velocity error $\dot{\tilde{\boldsymbol{q}}}$. With reference to the maximum value of the desired velocity (22) and (23), the corresponding velocity errors attain until 20% and 3.5%, respectively.

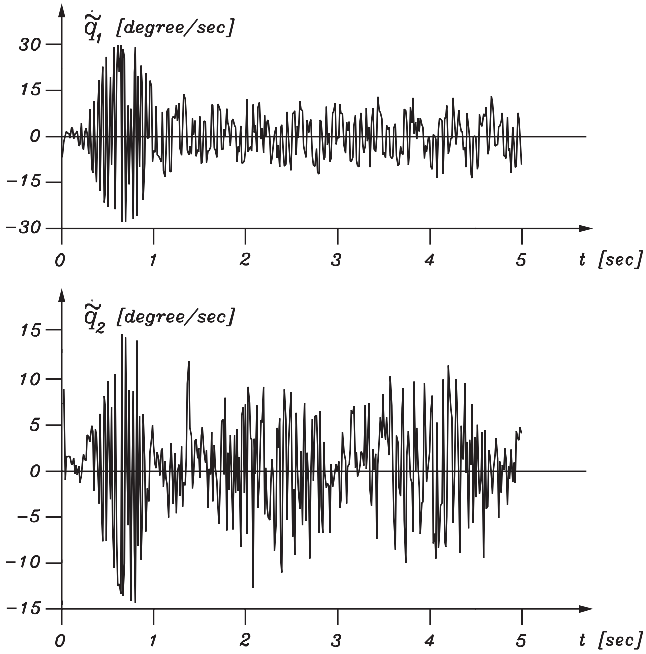

Figure 5. Joint velocity errors: inverse dynamics control.

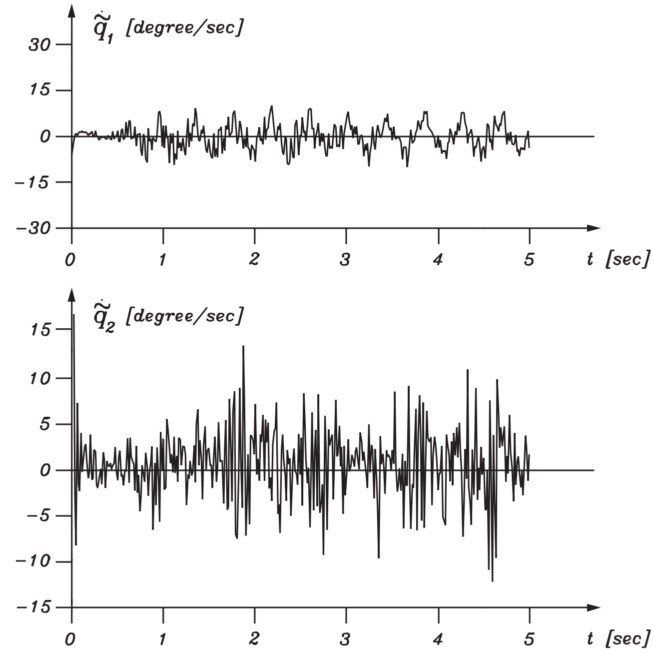

Figure 6. Joint velocity errors: PD control with compensation.

4.3. *PD control with compensation*

Experiments with the PD control with compensation (15) and (16) were conducted using the gains

$$K_i = \text{diag}\{1000, 1000\} \quad (\text{Nm/rad}) \tag{25}$$

$$K_v = \text{diag}\{63.25, 15\} \quad (\text{Nm s/rad}) \tag{26}$$

where the gain matrix Λ was

$$\Lambda = K_v^{-1} K_i = \text{diag}\{15.81, 66.66\} \quad (\text{s}^{-1})$$

Figure 6 depicts the velocity joint errors obtained from experiments. This figure shows a significant improvement in the reduction of velocity error $\dot{\tilde{q}}_1$ with reference to those in figure 5 obtained using the inverse dynamics control scheme. The maximum velocity errors are approximately 7% and 3.5%, respectively of the largest requested velocity.

4.4. *PD+ control*

The PD+ control scheme described by (18) and (19) was implemented using the same gain matrices (25) and (26).

The experimental results—joint velocity errors—are presented in figure 7. Compared with results of previous controllers shown in figures 5 and 6, the improvement is notable with regard to inverse dynamics control, but similar to the PD control with compensation.

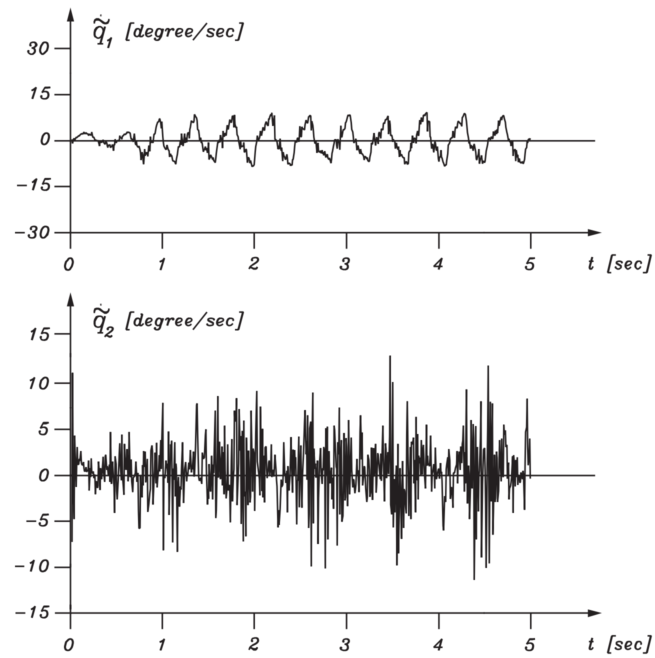

Figure 7. Joint velocity errors: PD+ control.

4.5. *Discussions*

Although global asymptotic stability implies that the velocity error $\dot{\tilde{\boldsymbol{q}}}$ must vanish asymptotically, in practice figures 5–7 reveal the existence of a steady state oscillatory behaviour. This is due to several factors such as uncompensated Coulomb friction, discrete controller implementation, and estimation of joint velocity via numerical differentiation of the joint position.

Visual examination of figures 5–7 is not suitable for quantitative description of velocity tracking errors, but

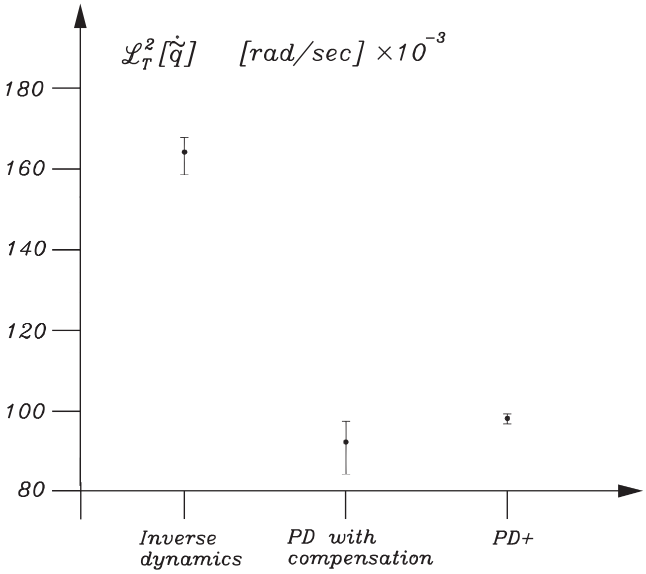

Figure 8. Performance based on $\mathcal{L}_T^2[\dot{\tilde{\boldsymbol{q}}}]$ truncated norm.

the $\mathcal{L}_T^2$ truncated norm criterion gives a useful performance index as shown in figure 8. To average out stochastic influences, the data presentation in this figure represents the mean of root-mean-square velocity error vector norm of ten runs.

The velocity controller based on the PD control with compensation had the best performance compared with the PD+ and the inverse dynamics controllers. Although the former had the bigger variation of the $\mathcal{L}_T^2$ criterion, the average was the smaller one. The PD+ control had better repeatability but the average was lightly larger than the PD control with compensation. Finally, the inverse dynamics based velocity controller presented the worst $\mathcal{L}_T^2$ average. This result is not surprising because the inverse dynamics technique is less robust to parameter uncertainty which can cause imperfect cancellation and hence poor performance than the PD control with compensation and the PD+ control which are passivity-based controllers.

5. Concluding remarks

This paper has dealt with joint velocity control of robotic manipulators. Three model-based motion control schemes (joint position tracking controllers) have been adapted to formulation of joint velocity control. Such control schemes are the inverse dynamics technique, the PD+ control and the PD control with compensation. The modification of these control strategies has been motivated by the well-known PI feedback structure utilized for velocity control of DC motors. In summary, the joint position error in the motion controllers has been replaced by an integral action of the joint velocity error; in this way, these controllers have an inner PI feedback velocity loop similar to that used for speed control of DC motors.

The feasibility of these velocity control schemes has been tested on a two degree-of-freedom direct-drive arm where the non-linear dynamics cannot be neglected. The controller based on the PD control with compensation appears to behave better.

Acknowledgements

The authors would like to thank the partial support of CONACyT, SNI, and CYTED.

References

Asada, H., Kanade, T., and Takeyama, I., 1983, Control of a direct-drive arm. *Transactions of the ASME, Journal of Dynamic Systems, Measurement and Control*, **105**, 136–142.

Bonivento, C., Nersisian, A., Tonielli, A., and Zanasi, R., 1994, A cascade structure for robust control design. *IEEE Transactions on Automatic Control*, **39**, 846–849.

Canudas de Wit, C., Siciliano, B., and Bastin, G., 1996, *Theory of Robot Control* (London: Springer-Verlag)

Corke, P., 1994, The Unimation Puma Servo System. MTM-226 report, CSIRO Division of Manufacturing Technology, Australia.

De Jager, B., and Banens, J., 1994, Experimental evaluations of robot controllers. *Proceedings of the 33rd IEEE Conference on Decision and Control*, Lake Buena Vista, FL, USA, December, pp. 363–368.

De Schutter, H. Bruyninckx, W. H. Zhu, and M. W. Spong, 1997, Force control: A bird's eye view. In B. Siciliano and K. P. Valavanis (Eds) *Control Problems in Robotics and Automation*, Lecture Notes in Control and Information Science 230 (London: Springer-Verlag).

Han, S. H., Kim, Y. H., and Ha, I. J., 1998, Iterative identification of state-dependent disturbance torque for high-precision velocity control of servo motors. *IEEE Transactions on Automatic Control*, **43**, 724–729.

Jaritz, A., and Spong, M., 1996, An experimental comparison of robust control algorithms on a direct drive manipulator. *IEEE Transactions on Control Systems Technology*, **4**, 627–640.

Kim, K. C., Ortega, R., Charara, A., and Vilain, J. P., 1997, Theoretical and experimental comparison of two nonlinear controllers for current-fed induction motors. *IEEE Transactions on Control Systems Technology*, **5**, 338–348.

Koditschek, D., 1984, Natural motion for robot arms. *Proceedings of the 23rd IEEE Conference on Decision and Control*, Las Vegas, NV, USA, December, pp. 733–735.

Kuo, B. C., 1982, *Automatic Control Systems*, 4th edn (Englewood Cliffs, NJ: Prentice-Hall).

Luh, I. Y. S., 1983, Conventional controller design for industrial robots—A tutorial. *IEEE Transactions on Systems, Man, and Cybernetics*, **SMC-13**, 298–316.

Nilsson, K., 1996, Industrial robot programming. PhD thesis, Department of Automatic Control, Lund Institute of Technology, Sweden.

Ogata, K., 1970, *Modern Control Engineering* (Englewood Cliffs, NJ: Prentice-Hall).

Reyes, F., and Kelly, R., 1997, Experimental evaluation of identification schemes on a direct drive robot. *Robotica*, **15**, 563–571.

Reyes, F., and Kelly, R., 2001, Experimental evaluation of model-based controllers on a direct-drive robot arm. *Mechatronics*, **11**, 267–282.

Santibañez, V., and Kelly, R., 1997, Strict Lyapunov functions for control of robot manipulators. *Automatica*, **33**, 675–682.

Slotine, J. J., and Li, W., 1991, *Applied Nonlinear Control* (Englewood Cliffs, NJ: Prentice-Hall).

Spong, M., Ortega, R., and Kelly, R., 1990, Comments on 'Adaptive manipulator control: A case of study'. *IEEE Transactions on Automatic Control*, **35**, 761–762.

Spong, M., and Vidyasagar, M., 1989, *Robot Dynamics and Control* (New York: Wiley).

Wen, J. T., and Bayard, D. S., 1988, New class of control law for robotic manipulator. Part 1: Non-adaptive case. *International Journal of Control*, **47**, 1361–1385.